ES&H DIVISION
RADIATION CONTROL DEPARTMENT

technical basis document

The Calculation of Neutron Skyshine Dose Rates at the TJNAF Fence Line

G. Stapleton

November 4, 1996

RCD-TBD-96 #001

originally published as JLAB-TN-96-061

Priority review level n/a

Document classification n/a

Next review due n/a

Submit for approval ☐ yes ☑ no

Thomas
Jefferson
National
Accelerator
Facility

Jefferson Lab
Thomas Jefferson National Accelerator Facility

Jefferson Lab Tech Note TN # 96-061
November 4, 1996

The Calculation of Neutron Skyshine Dose Rates at the TJNAF Fence Line

G. Stapleton

This tech note sets out the methodology developed in the early design stages of CEBAF for calculating the radiation dose rate at the laboratory boundary resulting from neutron skyshine arising from experiments in the end stations. This method is coded for computer processing as ELEC5a.

Introduction

A most demanding aspect of radiation protection at CEBAF is dealing with skyshine from the roofs of the end stations. The critical locations are the nearest points on the CEBAF boundary which must be controlled to an annual radiation dose equivalent less than 10 mrem (0.1 mSv). The radiation which dominates in skyshine is neutron radiation. The neutron dose equivalent due to natural background is rather low (approx. 4 - 5 mrem/year) so that utilizing event counting techniques $^{10}B(n,\alpha)^{7}Li$ or $^{3}He(n,p)^{3}H$ permits us to monitor say a doubling of normal background within a few hours.

Radiation protection is generally based on a calendar year so that we can derive a fixed maximum radiation budget at the fence post of a suitable fraction of the 10 mrem/year goal. We take 5 mrem/y as a budget for each end station A and C in the knowledge that we might want to overspend at the year end according to how the actual measurements correspond to estimates (calculation).

Calculation of the end station roof shielding was based on theoretical radiation sources in the end stations corresponding to the power of an electron beam impinging on a thick metal (iron) target at the center of the hall. This worked out to be approximately 40 W for one end station for a full year (365 days). In terms of deposited energy, this works out to be 1.26 10^{9} joules. It must be emphasized that this is for one end station, for two end stations operating (end station B can be ignored because it will use low intensity beams) then this deposited energy must be shared.

Types of Beam Loss in the End Stations

Beams loss occurs when the electron beam passes through the experiment target and any windows, "radiators", screens or gases used which can intercept the beam. These "thin" targets result in two kinds of beam loss phenomena; one is neutron production in the thin target by photons and electrons, and secondly the incident electrons can be scattered by the thin targets

into forward angles outside the "acceptance" of the beam dump channel to impinge on some component inside the end station.

Calculation of Thick Target Equivalent

Neutron Yield from Scattered Beam

In passing through the target and any radiators or windows the electrons will suffer multiple (small angle) or single (large angle) scattering. If the scattering angle is large enough the electrons will impinge on thick material around the beam line to produce a substantial radiation source. This mechanism can be simulated with a suitable Monte Carlo model but for rapid calculation we need a simple analytic representation of the scattering contribution.

The simplest seems to be to use a combination of the Gaussian and Rutherford single scattering expressions. Although other more refined treatments are available (Jenkins et al. 1969), the equation we adopt has the great virtue of simplicity and yet also matches rather well the results obtained by Monte Carlo calculations.

An approximate formula for the mean scattering angle for electrons proposed by Rossi (Rossi 1941 and 1952):

$$\langle \theta^2 \rangle = \left(\frac{E_s}{\beta p} \right)^2 t \qquad (1)$$

where
- E_s 21.2 MeV
- t thickness of scatterer (units of radiation length)
- βp particle momentum (approximately the same as kinetic energy E [MeV] for electrons at the energy of interest)

For Gaussian scattering, the probability of scattering into a space angle θ is given by:

$$P(\theta)d\theta = \frac{2}{\langle \theta^2 \rangle} \exp\left(-\frac{\theta^2}{\langle \theta^2 \rangle} \right) \theta d\theta \qquad (2)$$

Combining equations (1) and (2), the fraction of electrons, with no energy loss, multiply–scattered outside a cone half angle θ is given by:

$$g(\theta, t, E_0) = \frac{\int_\theta^\infty P(\theta)d\theta}{\int_0^\infty P(\theta)d\theta} = \exp\left(-\frac{\theta^2 E_0^2}{E_s^2 t} \right) \qquad (3)$$

converting $g(\theta, t, E_0)$ to beam power where I is beam current (μA) :

$$P_{sc}^{m} = E_0 I \exp\left(-\frac{\theta^2 E_0^2}{449.4t}\right) \text{(watts)} \quad (4)$$

At wider scattering angles the single scattering expression applies:

$$\frac{d\sigma}{d\omega} = \left(\frac{Zr_e m_e}{2p\beta}\right)^2 \frac{1}{\sin^4(\theta/2)} . R \text{ (cm}^2\text{ / sr.nucleus)} \quad (5)$$

where
- $d\omega$ interval in solid angle $\approx 2\pi \sin\theta\, d\theta$
- Z target charge number
- r_e classical radius of the electron ($2.818\ 10^{-13}$ cm)
- m_e electron rest energy (0.511 MeV)
- R correction term which can be ignored for small values of θ

Assuming $\sin\theta \cong \theta$ and integrating between θ and wider angles where $\sigma \cong 0$, we obtain:

$$\sigma = 4\pi\left(\frac{Zr_e m_e}{E_0\theta}\right)^2 \text{(cm}^2\text{ / nucleus)} = \frac{4\pi N_0}{A}\left(\frac{Zr_e m_e}{E_0\theta}\right)^2 \text{(cm}^2\text{ / g)} \quad (6)$$

where
- N_0 is Avogadro's number
- A is atomic weight of scatterer

and for a scatterer thickness t (radiation lengths) and radiation length X_0 (g/cm^2) equation (6) results in the expression for the fraction of electrons escaping a cone half angle θ:

$$\frac{0.157Z^2 tX_0}{AE_0^2\theta^2} \quad (7)$$

We can modify equation (7) to include a numerical fitting constant with respect to θ, introduced to give a value of $g(\theta,t,E_0)$ of unity when θ is zero:

$$g(\theta,t,E_0) = \frac{C}{\theta^2 + C} \quad (8)$$

where $$C = \frac{0.157Z^2 tX_0}{AE_0^2}$$

Thus an approximate fit to the power loss through single scattering is given by:

$$P_{sc}^{s} = E_0 I \frac{C}{\theta^2 + C} \text{ (watts)} \quad (9)$$

We can simply combine the two expressions (equations 4 and 9) by making the assumption that we are only concerned with the effect of multiple scattering on those electrons that are not

singly–scattered. We also replace Z^2 with Z(Z+4) intended to account approximately for the effect of electron scattering which becomes significant for low z targets such as hydrogen and deuterium (fit to Monte Carlo results):

$$P_{sc}^{m\&s} = E_0 I\left[\frac{C'}{\theta^2 + C'} + \left(1 - \frac{C'}{\theta^2 + C'}\right)\exp\left(-\frac{\theta^2 E_0^2}{449.4t}\right)\right] \tag{10}$$

where $$C' = \frac{0.157Z(Z+4)tX_0}{AE_0^2}$$

On comparing the above equation with results of Monte Carlo calculations we find very reasonable agreement. Figure 1 illustrates a typical comparison with Monte Carlo methods - it should be noted that the data in the figure are presented as derivatives of $P_{sc}^{m\&s}$.

In order to utilize this result for more than one beam insert, we assume that they are all combined into one scatterer located at a position determined by the ratio of the radiation length of the individual inserts (scatterers). For two inserts located at different positions in the beam line the position of the combined scatterer will lie nearer the thicker (in terms of radiation length) insert. For scatterers of thickness X_1, X_2, X_3 X_i.

$$\frac{X_{tot}}{X_0} = \frac{X_1}{X_{01}} + \frac{X_2}{X_{02}} + \frac{X_3}{X_{03}} + \cdots \frac{X_i}{X_{0i}} \tag{11}$$

where X_{tot}/X_0 is the thickness of the combined scatterer in radiation lengths
and X_i/X_{0i} is the thickness of the individual scatterers.

For an insert comprising more than one element we replace it with the the individual elements, scaled for thickness, as separate inserts located at the compound insert position.

Photo and Electro Production in Thin Targets

The basic expression we use in the code is a quotient in which the denominator is the thick (iron) target neutron yield and the numerator the thin target neutron yield. The resultant fraction is used to multiply the incident beam power to give the equivalent thick target radiation term.

For the denominator we estimate the photon differential track length using approximation A of shower theory (Rossi 1952) and combining with the production cross section we obtain:

$$0.572X_0^{Fe}E_0\int\frac{\sigma_{Fe}(k)}{k^2}dk \tag{12}$$

where k energy of photon in the reaction
X_0^{Fe} radiation length of iron
E_0 electron beam energy
$\sigma_{Fe}(k)$ photo production cross section for iron

For the numerator we have two cases:

Photoproduction In this case we use the simple thin target approximation:

$$\frac{t^2 X_0^T}{2}\int\frac{\sigma_T(k)}{k}dk \tag{13}$$

Electroproduction When electron beams are targeted on a large sized object of more than say a radiation length then electroproduction is negligible compared with photo production. However, for thin targets this is no longer the case so electroproduction must be included.

In this case we use a slightly more complicated method which utilizes the effective radiator thickness for virtual photon energy at given electron energies (Hyde-Wright et al. 1985). Figure 2 presents data from a calculation, using the equations of Hyde-Wright and his colleagues, as curves of t^v versus virtual photon energy for a series of electron beam energies extended upward from 1000 MeV to 10000 MeV. These equations are given in an appendix to this note.

Thus in the simple thin target approximation we obtain the virtual photon differential track length:

$$\frac{dl^v}{dk^v} = \frac{tX_0^T t^v}{k^v} \tag{14}$$

and the yield would be given by:

$$tX_0^T\int_{k_{min}}^{E_0}\frac{t^v\sigma_T(k^v)}{k^v}dk \tag{15}$$

The equations given by Hyde-Wright et al. (1985), enabled the simple generation of the integrals in equation (16) below, for the stated beam energies (E_0) and lower limit k_{min} = 100 MeV. A table of these integrals are used in ELEC5a with simple linear interpolations for intermediate beam energies.

$$\Psi(E_0) = \int_{k_{min}}^{E_0}\frac{t^v}{k^v}dk \tag{16}$$

Limits for the integrals Because the object of this calculation is to derive a factor which represents the fraction of the incident beam power incident on a thin target which produces approximately the same neutron fluence spectrum from a thick iron target we must be careful in the choice of the lower limit for the integral. Thick targets are much richer in lower energy

photons so if we choose too low a value for the lower limit, the quotient will produce a rather small value which will underestimate radiation levels, too high a value will be too conservative. Inspection of figures 4A and 4B will illustrate this concern. The figures show the photon track lengths for a thick target (approximation A of shower theory) for given beam energies (shown in the legend by the descriptor INT1/k^2), also shown are the photon track lengths for a thin target for both photoproduction and electroproduction again for given beam energies (shown in the legend by the descriptors PP-INT1/k and EP-INT1/k). The two figures correspond to two different thin target thicknesses: figure 1 A, being a rather thick "thin" target (10% X_0) and figure 1 B, a rather thin "thin" target (0.1%X_0). These figures clearly show the importance of electroproduction as a thin target source term, especially for very thin targets - illustrating the effect of the t^1 term in the electroproduction expression compared with the t^2 term in the photoproduction expression. Further inspection of these figures illustrates the options for choosing a lower integration limit. The choice of any energy below about 20 MeV would be inappropriate because we are only interested in neutrons with energy greater than about 20 MeV. Lower energy neutrons would be removed early in the transport process through thick roof shielding. To choose an energy much above 100 MeV would result in an unduly conservative result. Therefore, as a safe compromise we have chosen the lower limit to be 100 MeV, accepting that this could be reduced to 80 MeV or perhaps 50 MeV after obtaining actual measured results. The upper limit is the electron beam energy.

Photoproduction Cross Sections The basis for neutron production are the photonuclear cross sections shown in an approximate compilation by Degtyarenko reproduced in figure 5 (Degtyarenko 1995). In order to make a simplification of these data we began by listing the elements from figure 5 with their atomic weights in table 1 and, for three selected photon energies, their production cross sections as ratios to that of iron. In the last column of table 1 we have likewise listed the atomic weigh ratios of all the elements to that of iron. Inspection of these data show the very close correspondence of cross section ratios to that of the atomic weight ratios. This correspondence is further illustrated in figure 6. The value for deuterium lies below the line but this we simply corrected by dividing the derived cross section based on the atomic weight value by two.

Table 1. Cross section ratios (to Fe) and comparison with atomic weights

		total cross section ratio (elem/iron)			
elem	at wt	120 MeV	300 MeV	6000 MeV	at wt ratio
D	2	0.016	0.035	0.042	0.036
Be	9	0.145	0.146	0.151	0.161
C	12	0.210	0.192	0.189	0.214
Al	27	0.526	0.423	0.415	0.482
Fe	56	1.000	1.000	1.000	1.000
Cu	63	1.053	1.039	1.151	1.125
Pb	207	3.158	3.270	3.210	3.696

The complete quotient expression is given in equation (17) below for photoproduction (electroproduction would require the numerator to be based on equation (15) instead):

$$\frac{\frac{t^2 X_0^T N_0}{2A^T}\int_{100}^{E_0}\frac{\sigma_T(k)}{k}dk}{0.572\frac{X_0^{Fe}E_0N_0}{A^{Fe}}\int_{100}^{E_0}\frac{\sigma_{Fe}(k)}{k^2}dk} \qquad (17)$$

where
- t is thin target thickness (X/X_0)
- X_0^T is radiation length of target (g cm^{-2})
- X_0^{Fe} is radiation length of iron (g cm^{-2})
- N_0 is Avogadro's number
- A^T is atomic weight of target
- A^{Fe} is atomic weight of iron
- E_0 is beam energy (MeV)
- σ_T is photoneutron cross section for target (cm^2)
- σ_{Fe} is photoneutron cross section for iron (cm^2)
- k is photon energy (MeV)

However, we are able as a reasonable approximation to replace the values of σ_T and σ_{Fe} with the relevant atomic weights and canceling out equation (17) becomes:

$$\frac{\frac{t^2 X_0^T}{2}\int_{100}^{E_0}\frac{dk}{k}}{0.572X_0^{Fe}E_0\int_{100}^{E_0}\frac{dk}{k^2}} \qquad (18)$$

and for the electroproduction term:

$$\frac{tX_0^T\Psi}{0.572X_0^{Fe}E_0\int_{100}^{E_0}\frac{dk}{k^2}} \qquad (19)$$

where Ψ is the integral given by equation (16)

In order to check the validity of using a simple constant cross section in the quotients (18) and (19), a subroutine for generating cross sections for any value of photon energy was used for complete numerical integration for some example calculations. The results were in excellent agreement with the simplified method.

Calculation of Roof Shielding and Skyshine Dose Equivalent

We calculate the neutron dose rate on the roof using the SLAC method and it is given by the following equation, normalized to unit distance and for lateral shielding (90°):

$$H(t'') = Ae^{-t''/\lambda_A} + Be^{-t''/\lambda_B} + Ce^{-t''/\lambda_C} \qquad (20)$$

where t'' is the roof thickness

$\lambda_{A,B\&C}$ is the appropriate relaxation length

The appropriate quantities needed to solve this equation for beam energies above 1 GeV are given below in table 2. For lower beam energies, the source terms given by Sullivan (1992) are used. Sullivan's source terms are not constant with beam energy, so a tabulation (not included in this tech note) is used with linear interpolation for intermediate energies.
To convert H(t") to a neutron fluence, we apply a fluence to dose conversion coefficient D and the roof solid angle, assuming isotropy and constant shield thickness:

$$Q = H(t'') / D \qquad \text{(steradian}^{-1}\text{)}$$
$$Q_{tot} = H(t'')\Omega / D$$

Table 2. Constants for Shielding Equation

coefficient	rem GeV^{-1} e^{-1} cm^2	mrem h^{-1} W^{-1} cm^2	Sv h^{-1} W^{-1} m^2	$\lambda_{A,B,C}$ (g cm^2)
A	1.0 x 10^{-11}	2.25 x 10^5	2.25 x 10^{-1}	120
B	1.0 x 10^{-10}	2.25 x 10^6	2.25 x 10^{-3}	55
C	4.2 x 10^{-10}	9.45 x 10^6	9.45 x 10^{-3}	30

A roof which gives varying thicknesses over the angle from the source to the roof will require the thickness to be expressed as a function of angle and Ω would be obtained by numerical integration. The value of D we take from reference (Stapleton et al 1994). From the same reference we have the approximate expression for the skyshine dose at distance r from the center of the roof per spectrum average neutron:

$$H(r) = \frac{2\times 10^{-15}}{(r+40)^2}\exp\left(-r / \lambda_{sky}(E_0)\right) \text{ (Sv neutron}^{-1}\text{)} \qquad (21)$$

where r is horizontal distance from skyshine source (m)

$\lambda_{sky}(E_0)$ is an exponential transmission factor for the radiation which varies with primary electron beam energy. Its value is found from reference (Stapleton et al 1994).

Values of D and λ_{sky} are presented in tables 3 and 4 for selected values of E_0. these data are interpolated for intermediate energies.

Table 3.

E_0 (MeV)	400.	630.	1000.	1600.	2500.	4000.	6300.
D ($fSvm^2$)	13.2	13.7	14.1	14.4	14.5	14.6	14.6

Table 4.

E_0 (MeV)	400.	1000.	3000.	5000.	6000.
λ_{sky} (E_0) (m)	492.	570.	641.	656.	656.

Conclusions

The results of using this method of calculation have been compared with measurements in the field. The results so far obtained show that the method is reasonable and with very little additional tuning should provide a reasonably quick method of estimating to an accuracy of about (20% - 30%) the likely dose rates at the facility fence line. However, it must be clearly stated that the best approach is to model the set-up using a suitable Monte Carlo transport code in conjunction with an appropriate event generator such as DINREG. DINREG is currently under development at Jlab (Degtyarenko 1995).

Acknowledgments

The author acknowledges the help given him by Peter Kloeppel and also to Mike Finn, Lew Keller and Roy Whitney who showed the way of dealing with the intricacies of electroproduction. The later help of Pavel Degtyarenko, especially for his γA cross section curves and the external function which generates them, is also gratefully acknowledged.

References

Degtyarenko, P.; Applications of the Photonuclear Fragmentation Model to Radiation Protection Problems. In: Shielding Aspects of Accelerators, Targets, and Irradiation Facilities (SATIF2). Proceedings of OECD Nuclear Energy Agency Second Specialist's Meeting. CERN, Geneva, Switzerland; October 1995: 67-91.

Hyde-Wright, C. E.; Bertozzi, W.; and Finn, J. M.; 1985 Summer Workshop, Ed. H. Crannell and F. Gross, CEBAF June 3-7 (1985)

Jenkins, T. M.; and Nelson, W. R.; The Effect of Target Scattering on the Shielding of High Energy Electron Beams, Health Phys. vol. 17, pp. 305–312, (1969).

Rossi, B.; and Greisen, K.; Rev Mod Phys vol. 13, 240, (1941)

Rossi, B.; High Energy Particles, Prentice - Hall, (1952)

Stapleton, G. B.; O'Brien, K.; and Thomas, R. H.; Accelerator Skyshine: Tyger Tyger Burning Bright, Part. Accel., Vol. 44(1) 1994.

Sullivan, A. H.; A Guide to Radiation and Radioactivity Levels Near High Energy Particle Accelerators, Nuclear Technology Publishing, (1992).

Appendix

Hyde-Wright et al. 1985, indicate that as an analogy with the real case of a spectrum of bremsstrahlung photons from a target of thickness t radiation lengths, which is given by: $\frac{d\Phi_\gamma}{d\omega} \approx \frac{t}{\omega}$ (photons per unit energy per incident electron), they could define a virtual target thickness t^v, such that:

$$\frac{t^v(e_1,\omega,\theta)}{\omega} = \int_{\Delta\Omega} d\Omega \Gamma(e_1,\omega,\theta)$$

In the appendix to their paper this function is given as follows:

$$\int_0^{4\pi\sin^2(\theta/2)} d\Omega\Gamma(e_1,\omega,\theta) = \frac{\alpha}{\pi\omega}\left[\begin{array}{l}\frac{e_1^2+e_2^2}{2e_1^2}\ln\left(\frac{4e_1^2e_2^2}{m^2\omega^2}\right)+\frac{e_1^2+e_2^2}{2e_1^2}\ln\left(\frac{m^2\omega^2}{4e_1^2e_2^2}+\sin^2\frac{\theta}{2}\right)- \\ \frac{e_2}{e_1}\sin^2\frac{\theta}{2}\left(\frac{m^2\omega^2}{4e_1^2e_2^2}+\sin^2\frac{\theta}{2}\right)^{-1}-\frac{(e_1+e_2)^2}{4e_1^2}\ln\left(1+4\frac{e_1e_2}{\omega^2}\sin^2\frac{\theta}{2}\right)\end{array}\right]$$

For the purposes of this present tech note we have slightly recast this equation as follows: for ω we use k^v, e_1 we use E_0, e_2 we use $E_0 - k^v$, and for $\sin^2(\theta/2)$ we use 1. From this equation we calculated the values of t^v given in figure 2.

$$t^v = \frac{\alpha}{\pi}\left[\begin{array}{l}\frac{E_0^2+(E_0-k^v)^2}{2E_0^2}\ln\left(\frac{4E_0^2(E_0-k^v)^2}{m^2(k^v)^2}\right)+\frac{E_0^2+(E_0-k^v)^2}{2E_0^2}\ln\left(\frac{m^2(k^v)^2}{4E_0^2(E_0-k^v)^2}+1\right) \\ -\frac{(E_0-k^v)}{E_0}\left(\frac{m^2(k^v)^2}{4E_0^2(E_0-k^v)^2}+1\right)^{-1}-\frac{(E_0+(E_0-k^v))^2}{4E_0^2}\ln\left(1+4\frac{E_0(E_0-k^v)}{(k^v)^2}\right)\end{array}\right]$$

In order to provide the integrals $\Psi(E_0)$ given in figure 3, the above equation was numerically integrated with respect to k^v:

$$\Psi(E_0) = \int_{k_{min}}^{E_0} \frac{\alpha dk}{\pi k^v} \left[\begin{array}{l} \frac{E_0^2 + (E_0 - k^v)^2}{2E_0^2} \ln\left(\frac{4E_0^2(E_0 - k^v)^2}{m^2(k^v)^2}\right) + \frac{E_0^2 + (E_0 - k^v)^2}{2E_0^2} \ln\left(\frac{m^2(k^v)^2}{4E_0^2(E_0 - k^v)^2} + 1\right) \\ -\frac{(E_0 - k^v)}{E_0}\left(\frac{m^2(k^v)^2}{4E_0^2(E_0 - k^v)^2} + 1\right)^{-1} - \frac{(E_0 + (E_0 - k^v))^2}{4E_0^2} \ln\left(1 + 4\frac{E_0(E_0 - k^v)}{(k^v)^2}\right) \end{array} \right]$$

As pointed out by Hyde-Wright et al. the first term is dominant and other terms are small additions.

Figure 1. Electron scattering by 2% r.l. iron target

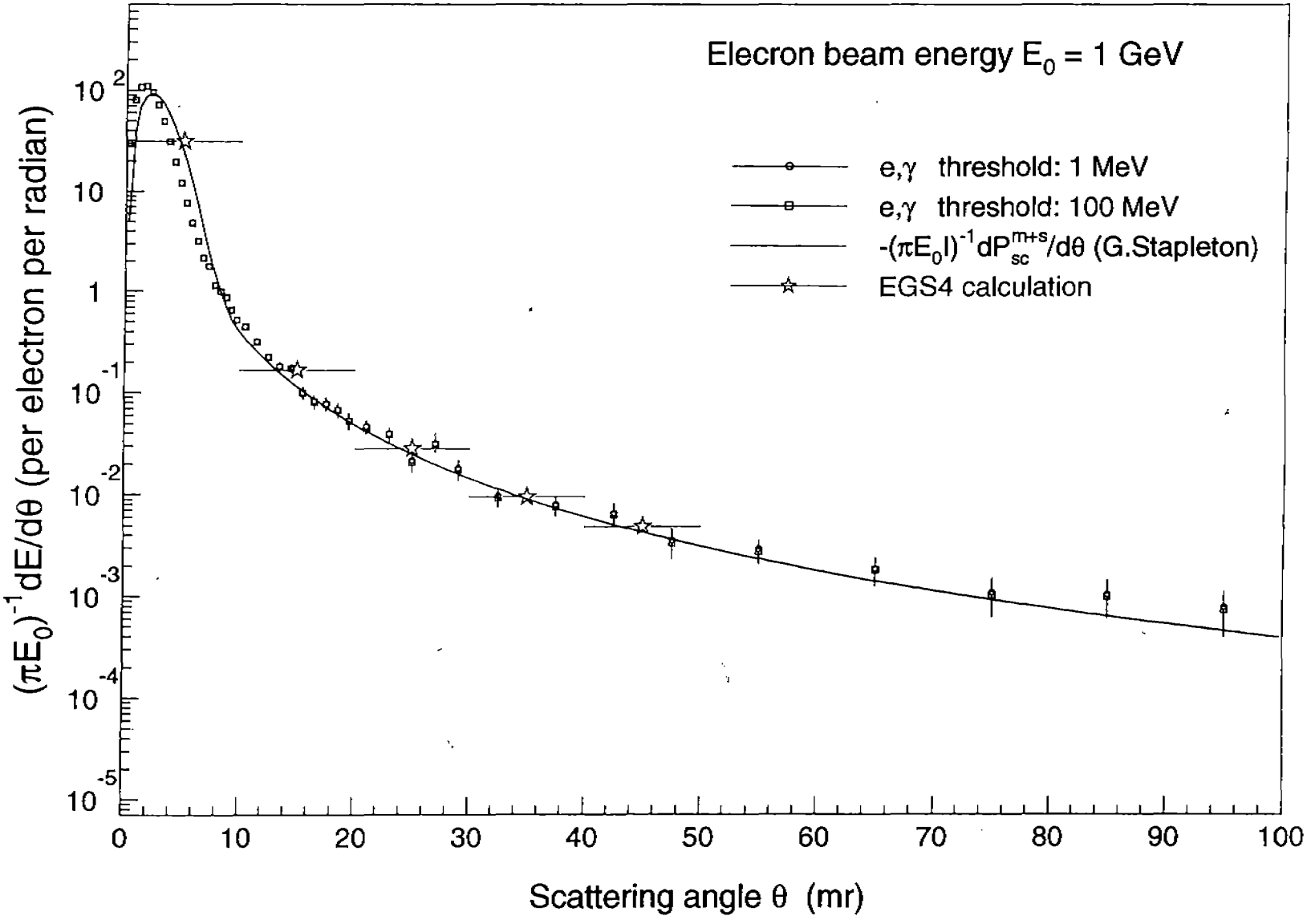

Figure 2. virtual photon radiator thickness vs. vitual photon energy for stated beam energies in legend (MeV) [after Hyde-Wright et al. 1985]

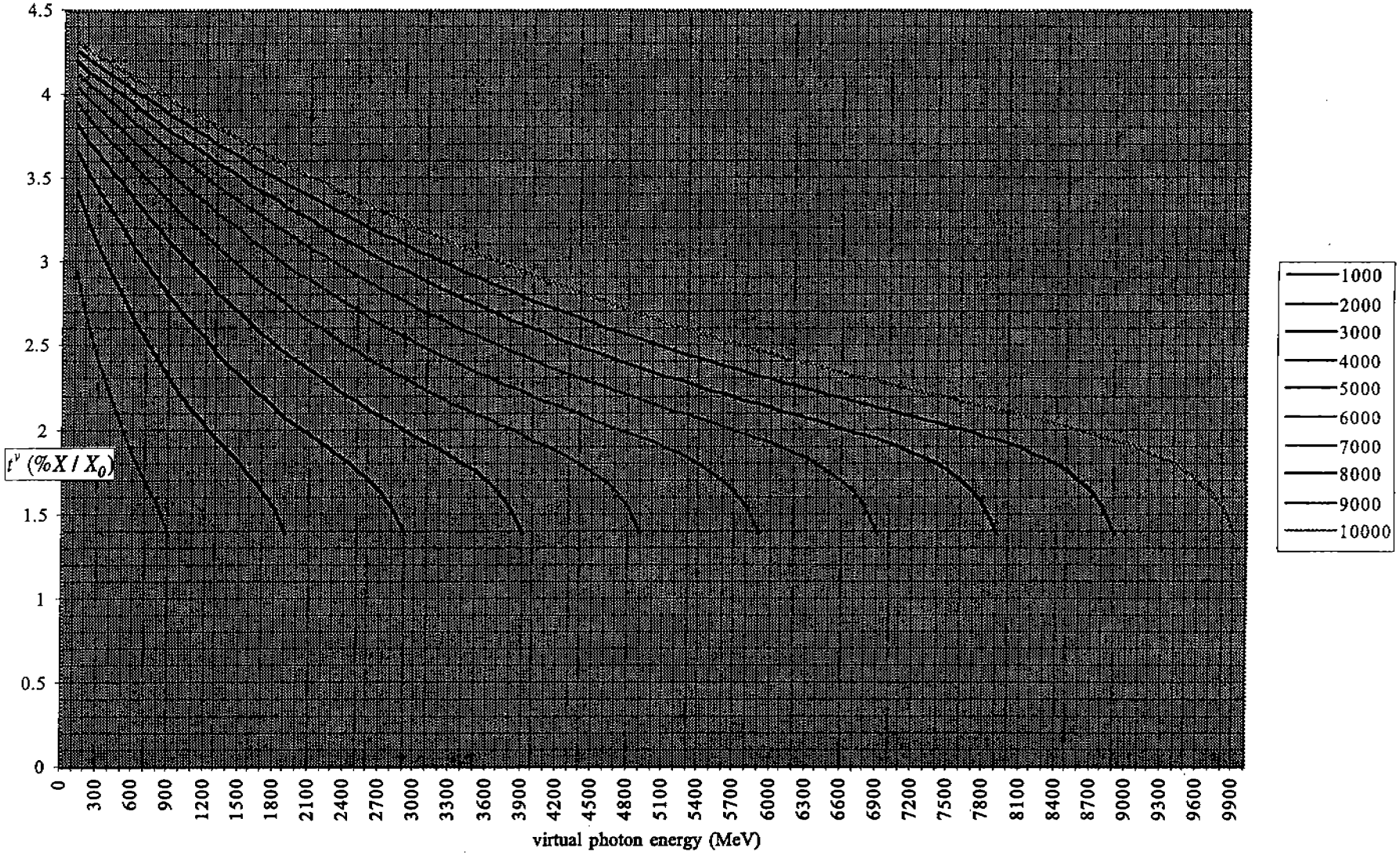

Figure 3. integral (equ'n 16) vs. electron beam energy

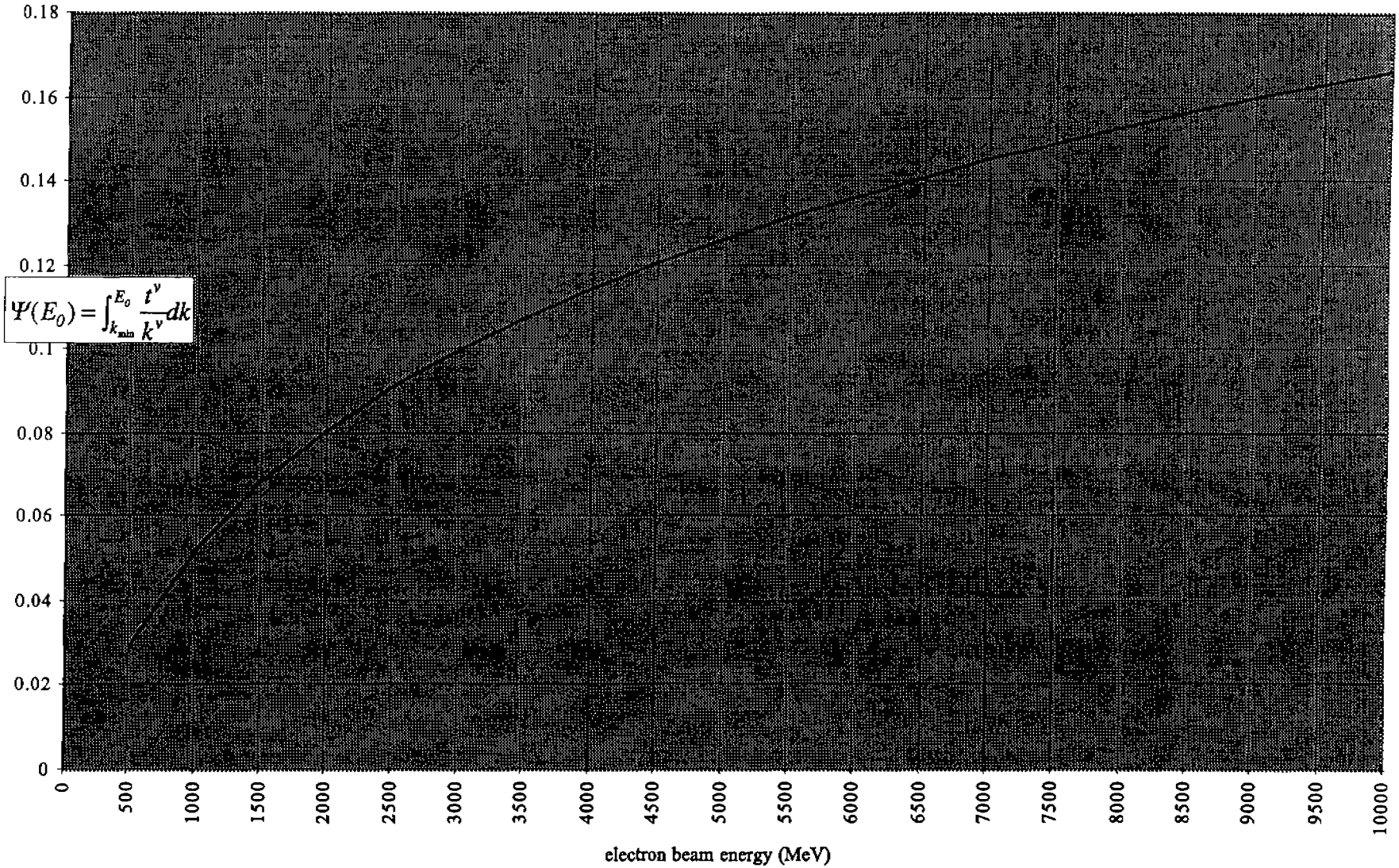

Figure 4A. photon track length integrals vs. lower integration limit [legend–beam energy (MeV), thick target (1/k^2) & thin (10%) target (1/k), phot prod (PP), elec prod (EP)]

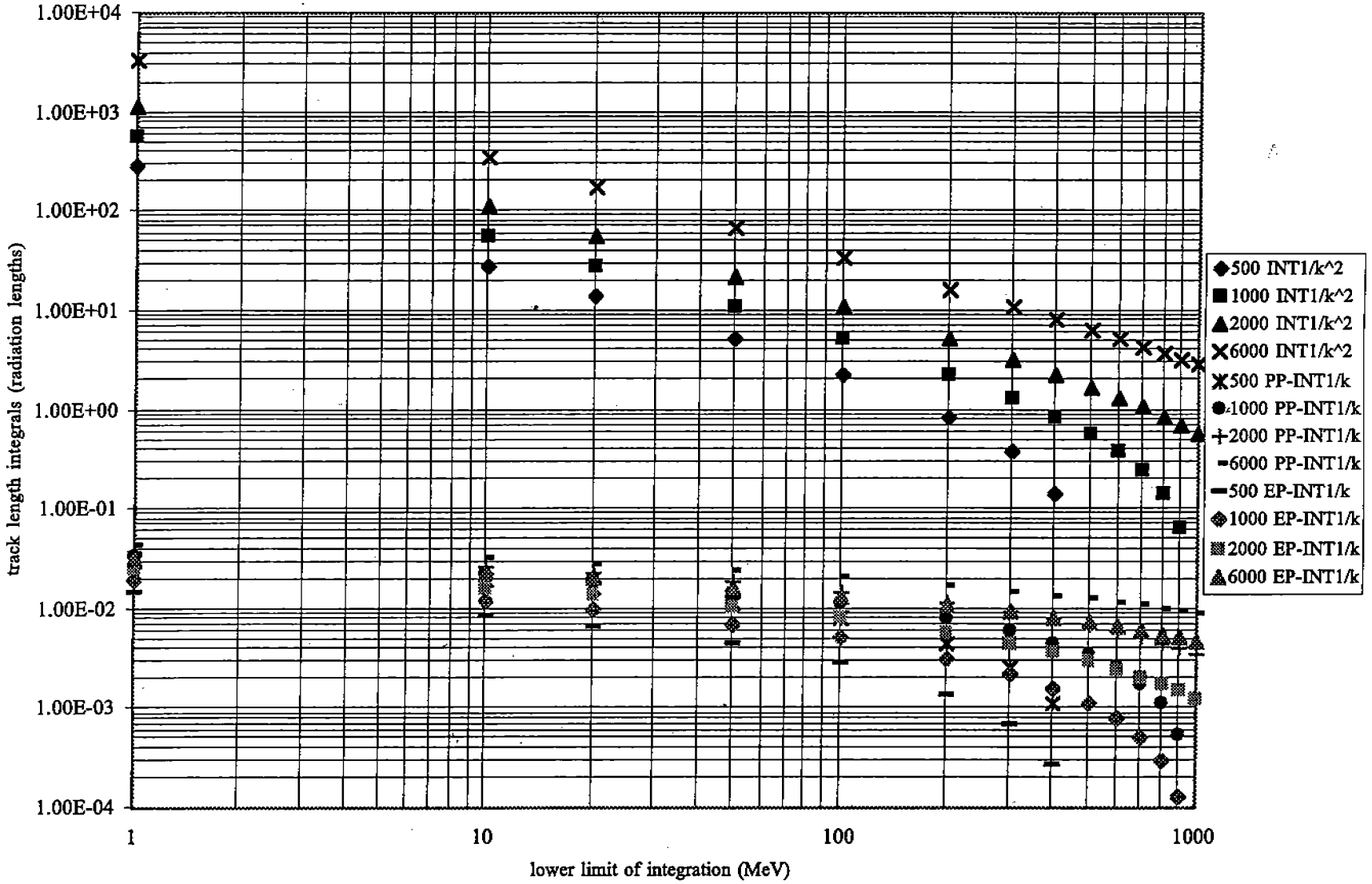

Figure 4B. photon track length integrals vs. lower integration limit [legend–beam energy (MeV), thick target (1/k^2) & thin (0.1%Xo) target (1/k), phot prod (PP), elec prod (EP)]

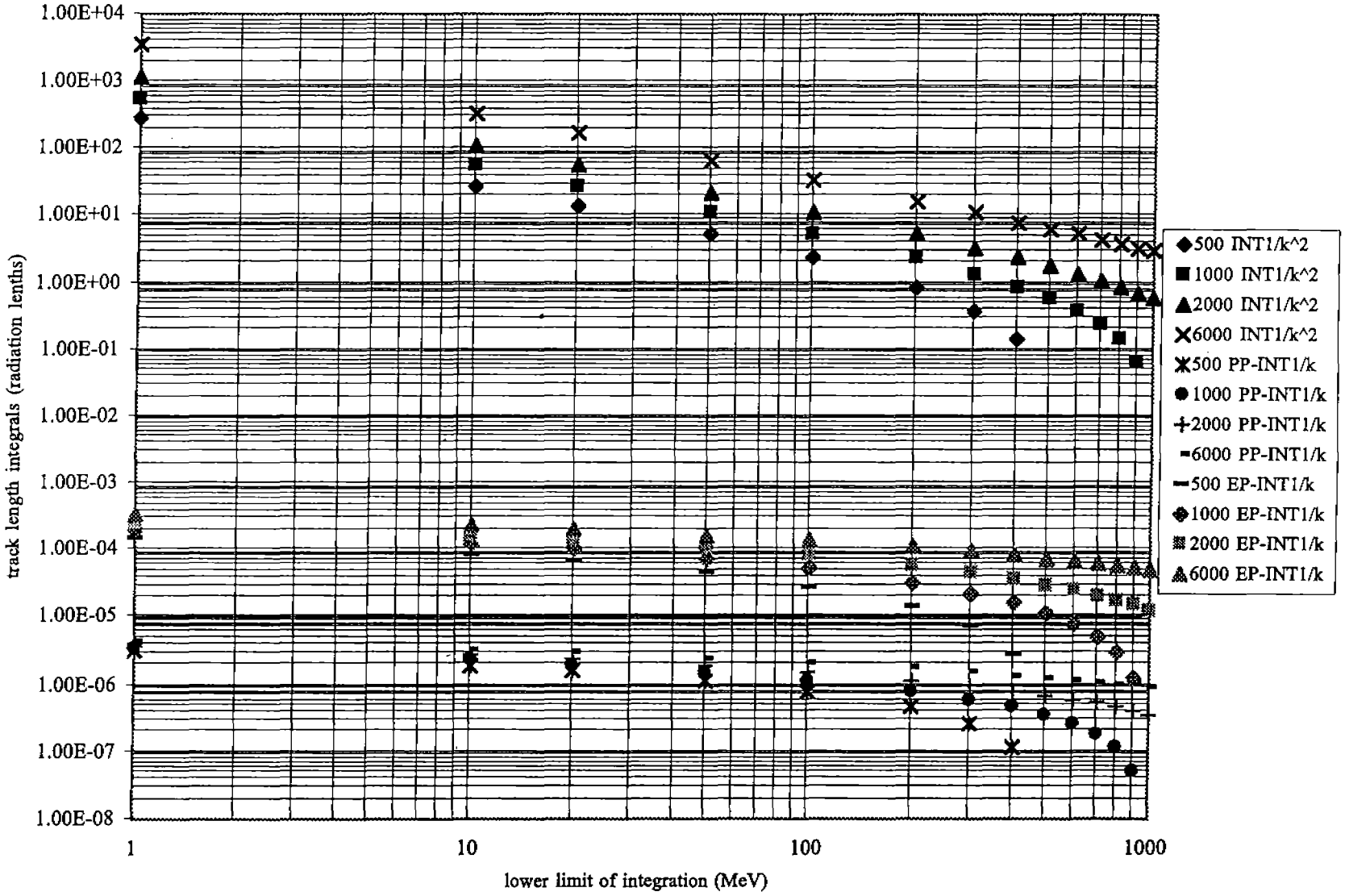

Figure 5. Photonuclear cross sections

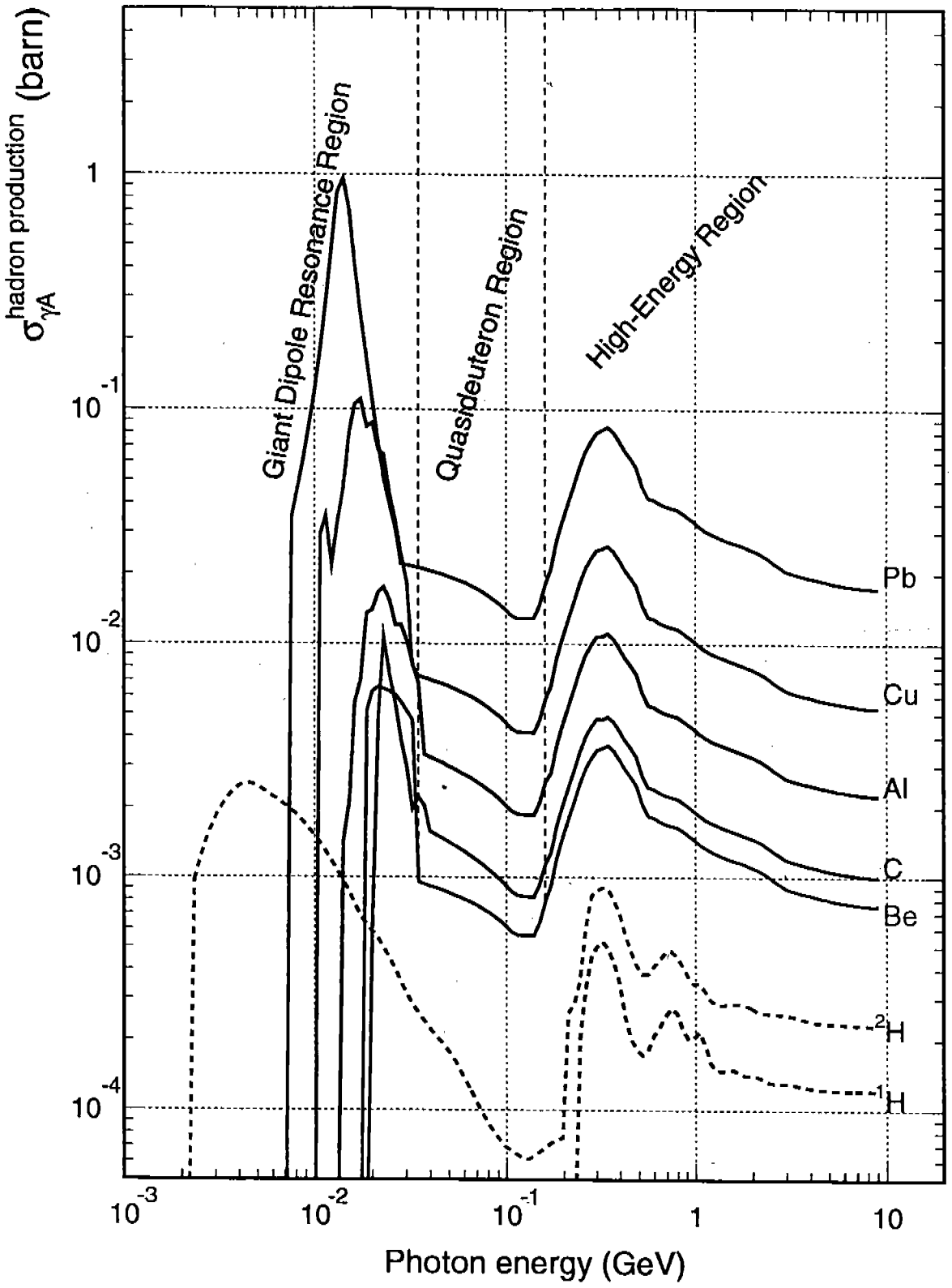

Figure 6. photonuclear cross sections vs. atomic weight